Key Enablers for Extreme MIMO Antennas and Receivers in Future 6G Frequency Bands

Padmanava Sen, Merve Tascioglu Yalcinkaya, Sourya Prakash Rout

Barkhausen Institut, Dresden, Germany
{padmanava.sen|merve.tascioglu|sourya.rout}@barkhauseninstitut.org

***Abstract*—The sixth generation (6G) networks are in their early development stage, with new technologies and frequency bands being currently considered. The enablement of extreme multiple-input multiple-output (xMIMO) will be of paramount importance to address the multi-user support requirements. In this work, we investigate the enabling components for such a system with a focus on the receiver front-end and antennas. Specific solutions are proposed and validated with simulations to mitigate the challenges of adding many elements in the multiple-input multiple-output (MIMO) systems. Special considerations are taken to design a mixer-first receiver at the 7-15 GHz frequencies targeting Frequency Range 3 (FR3) usage in 6G. The antenna performance parameters are analyzed using an open-source simulator, and the proposed designs with mutual coupling suppression are compared with traditional designs using Electromagnetic (EM) tools.**

***Index Terms*—antenna, MIMO, front-end, beamforming, receiver.**

I. Introduction

In the evolution toward sixth generation (6G) networks, communication systems are expected to simultaneously deliver high data rates, ultra-low latency, and reliable connectivity to multiple users [1]. This challenge becomes especially complex in the FR3 band (7–15 GHz), where bandwidth is moderate, and propagation losses are higher than in sub-6 GHz. Nevertheless, the wavelength is short enough to accommodate large antenna arrays. While multiple-input multiple-output (MIMO) is an integral part of current fifth generation (5G) systems, the future generation of mobile networks will work towards increasing the number of elements and use the new bands, namely frequency range 3 (FR3) [2]. Since the introduction of MIMO systems in the early 1990s, the demand for an increasing number of elements and support for more users is primarily triggered by exponential growth in data demand, connection density requirements, additional applications, and continuous addition of new users [3]. While extremely large multiple-input multiple-output (XL-MIMO) systems [4] mostly consider large physical array size, extreme multiple-input multiple-output (xMIMO) has broader potential industry usage, including XL-MIMO, cell-free, and distributed MIMO. This paper will primarily consider the radio frequency (RF) hardware challenges, namely transceiver and antenna/beamforming options with an increasing number of elements for an xMIMO system.

This work is financed with tax revenue on the basis of the budget approved by the Saxon state parliament.

Apart from supporting xMIMO systems, the future transceivers also need to be reconfigurable and adaptive to meet the dynamic needs of power per element and number of elements. Within the next 5-10 years, we will need an adaptive transceiver that can support the increasing trend of more elements as well as smaller form factors to fit the antennas. Given 7–15 GHz band antennas will be larger than that in mmWave, and the array gain achievable can be limited by the number of elements or the individual antenna element gain, the power-performance-area optimization of transceiver blocks will be a key decisive factor while considering the different bands to support in FR3. Identifying the performance-degrading factors/bottlenecks in such a system and mitigating them with innovative solutions will be the key objective of this paper, with a focus on receiver and antenna array designs. The main contributions of this paper are given below:

- Analysis of the challenges for increasing elements in MIMO systems;
- Next generation reconfigurable receiver solutions to mitigate the wideband receiver challenges;
- Antenna solutions to accommodate more elements while considering the mutual coupling and wideband operation requirements.

Energy optimization and embedding intelligence into systems and networks are also gaining significant interest with the introduction of deep learning based optimization [5]. Providing more services without increasing energy usage is a key topic discussed in 6G platforms. Reconfigurability in RF hardware is projected as a key enabler for future sustainable systems with context and energy awareness. The multi-purpose systems also need to enable different application needs, namely, integrated sensing and communication (ISAC). While embedding active radar sensing functionality into future xMIMO systems will make them smarter and energy efficient with context awareness, it will also add antenna and transceiver front-end challenges, especially in terms of self-interference cancellation (SIC). The mutual coupling among elements and finding additional antenna resources for the radar receiver will be an added requirement for ISAC.

Section II details the RF transceiver front-end and beamforming options. Section III considers a scalable solution to enable wideband receivers. Section IV highlights the different challenges and solutions for wideband and large arrays. Sec-

tion V discusses the findings from the designs, and Section VI concludes the paper.

II. RF Architecture

In this section, beamforming options and transceiver architectures will be investigated. The RF hardware challenges for xMIMO system can be summarized as:

- achieving wideband antenna operation while addressing antenna gain and element-to-element coupling with limited separation and low-cost packaging;
- fitting the power budget of transmitter and receiver while meeting the gain, linearity, wideband operation, and low noise performances, and the package to support it;
- accurate calibration considering the hardware imperfections between elements in different frequency ranges.

A complete analysis of xMIMO systems in terms of transmitter, receiver, antennas, analog to digital converter (ADC), digital to analog converter (DAC), and signal processing is beyond the scope of this specific work. In this work, antenna and receiver challenges are discussed and mitigated with designs presented in the paper.

A. Beamforming Options

To fully exploit the spatial resolution offered by short wavelengths in the FR3 band, beamforming techniques capable of precise directional control are essential to overcome propagation loss, and to support high user densities. However, two conventional approaches, analog and fully digital beamforming, face fundamental trade-offs, as shown in Fig. 1 [6].

Analog beamforming is limited to single-stream transmission, making it unsuitable for multi-user MIMO. Also, the phase shifters can lead to beam squint where the main beam direction shifts with frequency variation. Therefore, analog beamforming is inappropriate for the targeted FR3 band [7], [8] with a wide bandwidth. Conversely, digital beamforming provides precise spatial control with flexibility while realizing phase shifts in the digital domain. It supports many simultaneous users but requires an RF chain per element, DAC for every antenna at the transmitter, and ADC at the receiver [9], [10]. This leads to unscalable power consumption, heat dissipation, and cost in large arrays. This tension between performance and hardware feasibility presents a key barrier to implementing xMIMO in the FR3 band.

To resolve this trade-off, hybrid beamforming has emerged as a promising architecture for scalable 6G systems. It strategically combines analog and digital processing to support multi-user communication with significantly fewer RF chains than antenna elements, as shown in Fig. 1. Analog phase shifters are used to pre-steer beams, while digital baseband processing performs flexible precoding or combining across a smaller number of active RF paths. This structure offers near-digital performance with reduced power and hardware complexity, making it ideal for large antenna arrays typical in xMIMO. However, one notable issue previously identified is the reappearance of beam squint. Furthermore, hybrid beamforming introduces complexities in printed circuit board (PCB) layout and synchronization across subarrays due to integration of analog components with digital baseband processing. Hybrid beamforming may occasionally lead to degraded side lobes and phase inaccuracies when digital beams are directed away from the center of the analog beam, which can decrease overall gain [9]–[11]. Irrespective of these challenges, hybrid beamforming effectively balances energy efficiency, spatial multiplexing, and implementation feasibility, making it a strong candidate for 6G deployments operating in the $7-15\,\mathrm{GHz}$ band.

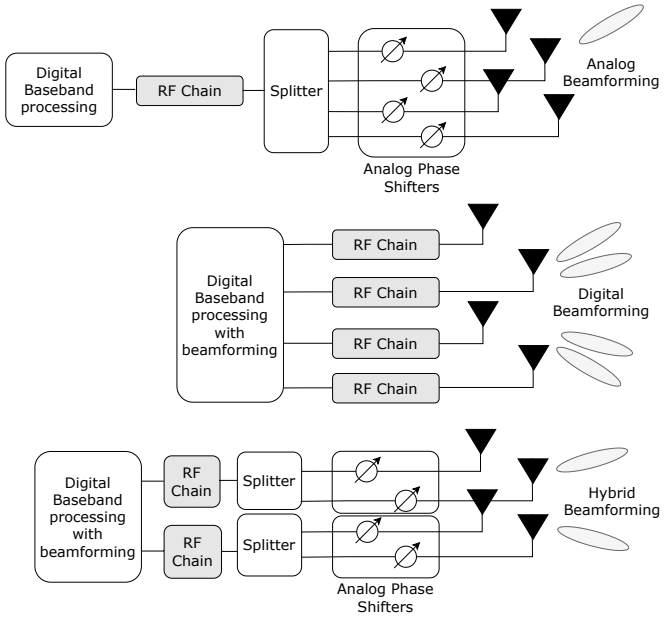

Fig. 1: Block diagram showing analog, digital, and hybrid beamforming architectures.

Other strategies, such as switched and adaptive beamforming, offer benefits in specific scenarios. Switched beamforming uses predefined beam codebooks, which makes them simpler but lacks spatial resolution and multi-user support. Adaptive beamforming can adapt to dynamic conditions, but it adds computational and feedback overhead. These limitations make both approaches less suitable for xMIMO systems [6].

Considering the three options, analog or hybrid beamforming may be more suitable to reduce power consumption if the goal is only to have a beamforming solution like that used in mmWave frequencies. If it is only about MIMO or Massive MIMO systems, the digital beamforming may have an edge over analog and hybrid options, especially to accommodate more users. However, in xMIMO with more elements, the power consumption of using different RF chains becomes the main bottleneck. In such a power-limited scenario, the hybrid beamforming becomes the preferred choice. However, the division between the number of chains and analog beamforming counterparts would depend on the frequency of operation, the number of users to support, the power budget, and the heat dissipation capacity of the package.

B. Transceiver Options

Considering a hybrid beamforming option, the power consumption of each transceiver block, including the phase shifters, becomes relevant in the realization of xMIMO transceiver. Given the limitations of the number of antennas per chain, the transmitter and receiver would need a switch to work in time division duplexing (TDD) mode, thus sharing the antenna between transmitter and receiver elements. Given at the FR3 bands, the switch loss will not be more than a few dBs, which can be absorbed in the link budget calculations. However, if an ISAC mode needs to be activated, that will demand some dedicated radar receivers with high isolation to the transmitters and an additional self-interference cancellation methodology. Also, in future 6G networks, dynamic switching of different elements based on resource requirements has been planned, which needs to be considered.

Even though the transmitter front-end is out of the scope of this paper, the main challenges and potential solutions are summarized for the transmitter below:

- hybrid beamforming to reduce the number of transmit chains and overall power consumption;
- application of digital predistortion (DPD) to manage the power amplifier (PA) nonlinearity in order to avoid operations at very low efficiency regions;
- individual power supply and bias switching to meet dynamic switching of chains, as well as to enable low power modes to provide flexibility in throughput;
- use of machine learning to calibrate hardware impairments, including amplitude/phase errors.

When selecting a receiver architecture for xMIMO systems in the FR3 band, several trade-offs arise between sensitivity, complexity, power consumption, and scalability. The conventional low noise amplifier (LNA)-first approach places an LNA directly after each antenna element to minimize noise and maximize sensitivity. While this architecture is effective for smaller arrays, it becomes increasingly inefficient in xMIMO systems due to the linear scaling of power consumption and the need for precise gain and phase calibration across a large number of analog chains. Furthermore, LNA-first receivers often rely on narrowband, resonance-based matching networks, which increase component count, occupy more area, and reduce frequency agility. Active mixer-first architectures offer some simplification by combining downconversion and gain. However, they still require biasing and resonant matching, leading to increased power and layout complexity that is problematic for dense, wideband implementations. Hence, a passive mixer-first approach is proposed in this work.

Section III will cover the proposed mixer-first solution for xMIMO receivers, considering the bandwidth, linearity, and power consumption as main key performance indicator (KPI) in a scalable architecture. Different antenna options are covered in Section IV. Given the requirement of compact implementations, the antenna system for xMIMO demands gain and isolation enhancement, while maintaining the compact size covering the different frequency bands.

III. Receiver topologies

Passive mixer-first receivers provide a scalable alternative. These architectures use switch-based passive mixers to enable direct RF-to-baseband downconversion without the requirements of active gain stages or bias circuits. In digital beamforming systems, passive mixers can be placed directly at the antenna interface, assisting wideband impedance matching through baseband impedance translation [12] [13]. In hybrid beamforming, however, analog combining precedes the mixer, and the bandwidth of the signal path is limited by the frequency response of analog components such as splitters and phase shifters. While the passive mixer remains capable of wideband operation, its full bandwidth advantage is only realized if the preceding beamforming network is also designed to be broadband. Although passive mixers exhibit higher intrinsic noise figures than active designs, the resulting noise penalty is largely mitigated in large array systems through array gain and noise averaging, which boosts the overall signal-to-noise ratio (SNR) [14] [15]. Passive mixers additionally provide high linearity that helps maintain signal integrity at the output of analog beamformers [13]. This characteristic is important as the spatial combination of signals can result in considerable dynamic range variations. Combined with their low power consumption and simplified layout, these attributes make passive mixer-first receivers well-suited for scalable, energy-efficient hybrid beamforming front-ends in 6G FR3 systems.

Fig. 2(a) shows the block diagram of a quadrature mixer-first receiver. The transistor switches act as passive mixers and are driven by non-overlapping square-wave pulses, generated by the quadrature local oscillator (LO) generator. The simulation results for input matching of a four-phase FR3 mixer-first receiver across swept LO frequency are shown in Fig. 2(b). The input matching is adaptable to changing LO frequencies, facilitating wideband operation and hardware reuse across the desired frequency range. The circuit is designed in Global Foundries 22nm Fully Depleted Silicon on Insulator (FDSOI) process, and the layout parasitic components are incorporated in the simulation results with the help of electromagnetic (EM) tools.

IV. Antenna topologies

In this section, the MIMO antenna is investigated with increasing number of elements. In recent decades, MIMO antenna systems have attracted significant interest in contemporary research due to their numerous advantages, including enhanced channel capacity, higher data rates, improved throughput, minimized signal attenuation, and reduced multipath fading. Despite its many merits, the primary challenge resides in designing the MIMO antenna, specifically in mitigating mutual coupling (MUC) among antenna elements and ensuring high levels of isolation [16], [17]. Generally, MIMO antennas are situated in close proximity. With an escalation in the number of elements (in the case of xMIMO, exceeding 64 elements), mutual coupling emerges as a significant issue.

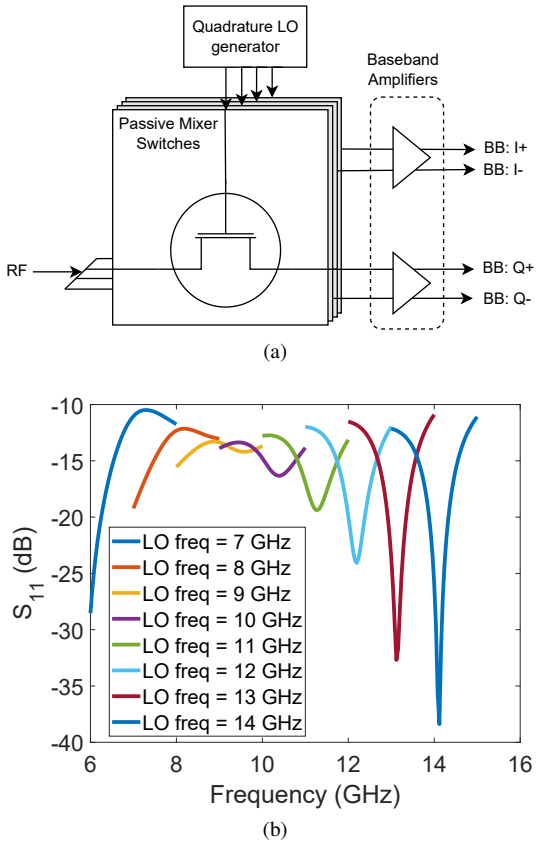

Fig. 2: (a) Block diagram of a quadrature mixer-first receiver (b) Input matching (S_{11}) of the FR3 receiver across swept LO frequency.

This mutual coupling results in:

1) distortion in radiation patterns,
2) impedance mismatches,
3) reduced isolation between elements.

A. Analysis with an increasing Number of Elements

This sub-section analyzes gain and side lobe level (SLL) using a Highly Portable Open Source Array & Phased Antenna Simulator, conceived at the Barkhausen Institute (BI). The tool incorporates an intuitive graphical user interface (GUI) that dynamically refreshes the simulation outcomes (visual representations) in accordance with alterations made by the user to the input parameters. Consequently, it emerges as a highly interactive tool, facilitating users in garnering significant insights pertaining to the subject matter of their interest. Comprehensive access to the scripts available in the GitHub repository [18], [19] enables the user to modify and enhance the instrument for specific applications. To investigate the mutual coupling effect on antennas, empirical models are commonly utilized to approximate the interaction between antennas and their performance parameters [16], [20], [21]. However, it may not always account for the surface waves, and thus for MUC, we have considered a design with and without an isolation boosting mechanism in the next sub-section.

Fig. 3 shows the gain variation with respect to the number of elements for different steering angles (θ), while maintaining a constant element spacing of $0.5\lambda_0$ where (λ_0) is the free-space wavelength. Since the spacing is defined in terms of the free-space wavelength, the mutual coupling effect is not explicitly considered. It should be noted that the guided wavelength (λ) is determined by the effective permittivity of the substrate, which determines the spacing between elements for antenna designs. Fig. 3 assumes a uniform array with identical elements, an ideal feeding network, fixed element spacing, and constant frequency operation. However, MUC alters the input impedance of each element, thereby inciting impedance mismatches. Such mismatches change the reflected power while concurrently diminishing the radiated power, which ultimately leads to a reduction in gain. In addition, MUC can perturb the current distribution, resulting in both constructive and destructive interference phenomena. While constructive interference has the potential to augment gain in specific orientations, destructive interference may diminish directivity, yield unforeseen side lobes, amplify the magnitude of pre-existing side lobes, or inhibit the main lobe.

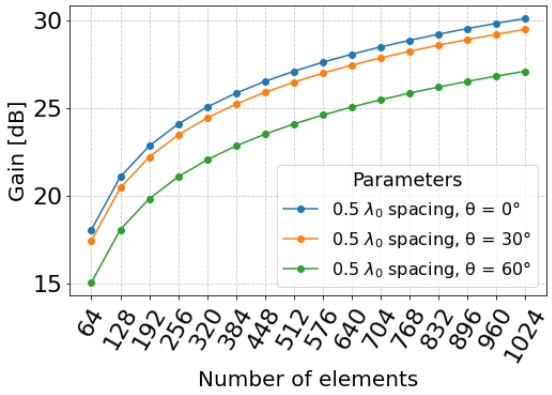

Fig. 3: Gain with respect to the number of elements (NOE).

Fig. 4 shows: (a) the implications of the number of elements, and (b) the influence of inter-element spacing on the performance of antennas. For the first case, three designs are considered with different elements: 16 x 16, 32 x 32, and 64 x 64, respectively. For the second case, three designs with different spacings are considered for 16 x 16 elements. It is distinctly observed that array configurations with inter-element spacing exceeding half a wavelength yield undesirable grating lobes. Moreover, the half-power beamwidth (HPBW) exhibits a reduction as the inter-element spacing expands. Fig. 4(a) illustrates that an increase in the number of elements is correlated with increased levels of the side lobe. The SLL may be attenuated to a specified degree through two well-established techniques: adjusting the amplitude of the elements' excitation or employing non-uniform element positioning [22]. Using the open-source simulator [7], non-uniform element positioning (symmetric inter-element spacing) is also examined. The SLL could be reduced, but at the cost of larger array sizes. Given that the total area of the antenna is a major concern for

xMIMO, this solution is not considered.

Fig. 4(b) illustrates the appearance of grating lobes, which occur when the element spacing is large relative to the wavelength. In such cases, the in-phase addition of radiated fields can occur in multiple directions. Grating lobes must be avoided in xMIMO systems, as they degrade directional selectivity and spatial resolution.

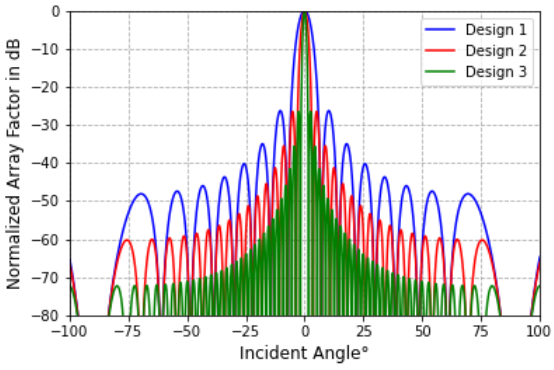

(a)

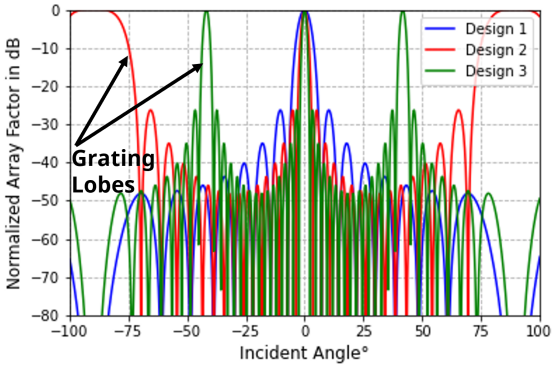

(b)

Fig. 4: Normalized array factor patterns of planar array (a) Effect of the NOE for Design1 - 16x16, Design2 - 32x32, Design3 - 64x64 elements with $0.5\lambda_0$ inter-element spacing, (b) Effect of different inter-element spacings for a 16×16 Planar Array for Design1 - $0.5\lambda_0$, Design2 - λ_0, Design3 - $1.5\lambda_0$.

B. EM-Wave Simulation of MIMO Antenna: Addressing MUC Challenges and Bandwidth Enhancement

Numerous scholarly articles examining strategies for enhancing MIMO antenna isolation have emerged in recent years. To mitigate mutual coupling and increase isolation, a variety of methodologies are employed, including neutralization lines, decoupling networks, parasitic structures, metamaterials, electromagnetic band gap (EBG) structures, and defected ground structure (DGS) configurations [17]. DGS offers a cost-efficient and easily manufacturable solution suitable for xMIMO applications. Furthermore, antennas operating in the 7-15 GHz frequency range typically exhibit omnidirectional radiation characteristics, making ultra-wide-band (UWB) designs suitable for MIMO applications. However, directive antennas can significantly enhance signal strength and extend communication range, crucial for supporting high-speed data transmission and mitigating the increased path loss at higher frequencies. To achieve both wide bandwidth and directional radiation, techniques such as patch slotting, the use of parasitic elements, or stacked configurations are commonly employed. In this paper, a slotted patch antenna design is analyzed and compared with a narrow bandwidth antenna. Fig. 5 presents a comparison between a narrowband rectangular patch antenna and an enhanced-bandwidth slotted patch antenna.

To analyze the NOE, arrays with different element counts were evaluated at an inter-element spacing of $0.5\lambda_0$. Fig. 6 illustrates a comparison between 2×2 and 4×4 planar array configurations. Accordingly, the observations from this result can be summarized as follows:

1) The higher NOEs in a large antenna array, the higher is the number of side lobes in the antenna pattern.
2) Regardless of the NOEs in an array, the first SLL exists at 13 dB below.
3) The higher the NOE, the smaller the beamwidth is.

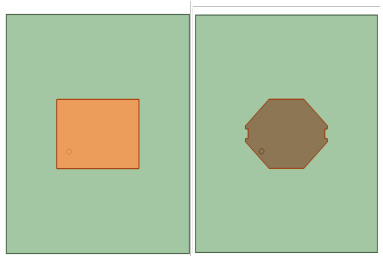

(a)

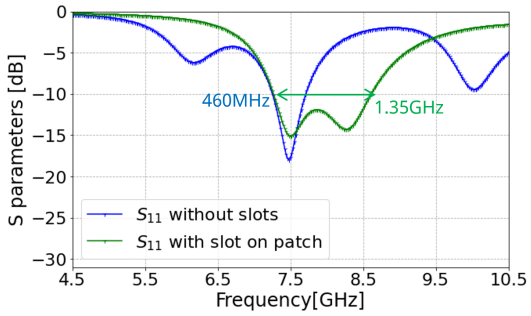

(b)

Fig. 5: Single element results - (a) Rectangular Patch antenna and Slotted Patch antenna, (b) Comparison of S parameter and 2D-Gain.

In an attempt to reduce the MUC in the proposed 2x2 planar array, DGS is implemented in between the antenna elements targeting the lower FR3 bands [2]: 7.125–8.4 GHz. During the design, the locations of the slots are optimized since they play a significant role in the performance of DGS structures. The proposed 2x2 planar array is designed on a low-cost Rogers substrate 5580 with a permittivity of 2.2 and a

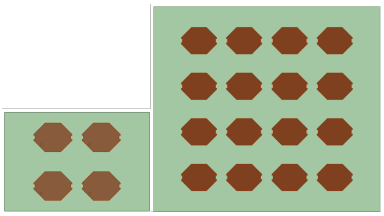

(a)

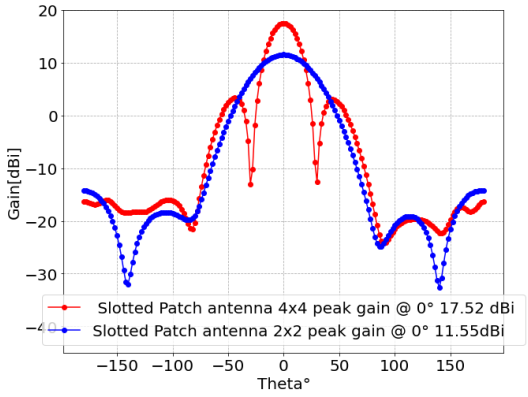

(b)

Fig. 6: Planar antenna results - (a) 2x2 Slotted Patch antenna and 4x4 Slotted Patch antenna, (b) Comparison of 2D-Gain.

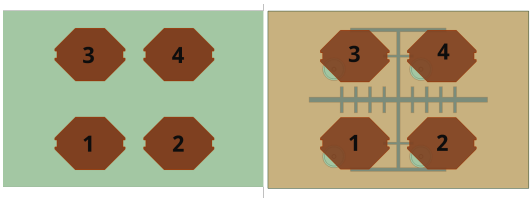

(a)

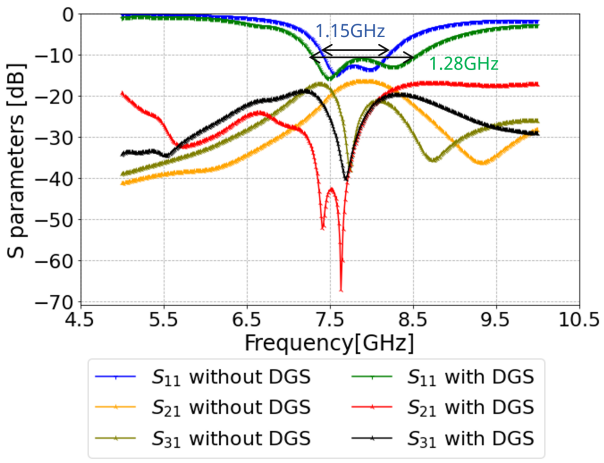

(b)

Fig. 7: Planar antenna results - (a) Planar antenna model without and with DGS, (b) Comparison of S parameters.

thickness of 1.575 mm. The geometrical layout of the proposed 2x2 planar array with DGS and without DGS is shown in Fig. 7(a). According to the simulation results, the proposed array with DGS has more bandwidth than the antenna array without DGS. This bandwidth enhancement is observed since the DGS on the ground increases the fringing field, increasing the parasitic capacitance. The 2x2 array without DGS shows a very strong coupling between antenna element 1 and antenna element 2, with an isolation value of 16.5 dB at the center frequency due to surface wave excitation. In addition, the coupling between antenna element 1 and antenna element 3 is minimal, primarily because their feed points are positioned far apart from each other. As a result, surface waves are suppressed and simulations show that peak isolation increases to 67 dB at 7.63 GHz, which is significantly higher than the antenna without the DGS counterpart, as illustrated in Fig. 7. The maximum gain of the antenna after integrating DGS is decreased from 11.55 dB (without DGS) to 11.29 dB (with DGS).

V. Discussions of Results

The theoretical analysis is performed for large arrays to investigate the impact of increasing elements. The reduction of MUC is also demonstrated using a 2x2 antenna with DGS in section IV. The EM simulation shows higher fractional bandwidth and better element-to-element isolation for the antenna with DGS. The proposed isolation boosting method (DGS) is scalable to a large number of elements. It also does not require special packaging methods and/or fabrication resolution like antenna solutions with EBG structures. The next step will be to investigate the possibility of multi-band antenna solutions to support additional bands in FR3 aligned with the wideband transceiver.

Section III demonstrated a mixer-first design that can work for multiple FR3 bands. When carefully co-designed, passive mixer-first receivers and hybrid beamforming architectures complement each other well, offering a highly scalable and energy-efficient solution for xMIMO systems in the FR3 band. Hybrid beamforming addresses the RF-chain scalability challenge, while passive mixers simplify the front-end with minimal power and excellent linearity, making the combination particularly effective for next-generation 6G receiver design.

Both mixer-first receiver and DGS-boosted antennas are proven to be key enablers for xMIMO. The next step is to conduct a thorough analysis of the power, performance, and area in a TDD transceiver considering hybrid beamforming, along with DGS-boosted large antenna arrays.

VI. Conclusion and Future Work

This paper discusses the challenges of RF transceiver and antenna implementation for xMIMO systems and potential solutions to mitigate them. Different enablers, namely, mixer-first receivers and isolated wideband antenna designs, are highlighted towards a scalable architecture of xMIMO systems. The antenna scalability is analyzed using an antenna simulator. As future work, the transmitter and phase shifting solutions could be included in the RF hardware development, leading to an optimum hybrid beamforming solution for a large

number of elements. From an Antenna point of view, different wideband versus multi-band antennas could be compared with the total area and element-to-element spacing in mind.

REFERENCES

[1] H. Holma, H. Viswanathan, and P. Mogensen, "Extreme Massive MIMO for Macro Cell Capacity Boost in 5G-Advanced and 6G," White Paper 210786, Nokia, 2021. Accessed: Jul. 14, 2025.

[2] Nokia, "6G Mid-Band Spectrum Technology Explained." https://www.nokia.com/6g/6g-mid-band-spectrum-technology-explained/. Accessed: 2025-07-14.

[3] A. Musa, P. O. Balogun, and A. O. Adebayo, *Applications of Massive MIMO in Wireless Communication Systems*, ch. 3, pp. 59–94. John Wiley Sons, Ltd, 2025.

[4] Z. Wang, J. Zhang, H. Du, D. Niyato, S. Cui, B. Ai, M. Debbah, K. B. Letaief, and H. V. Poor, "A tutorial on extremely large-scale mimo for 6g: Fundamentals, signal processing, and applications," *IEEE Communications Surveys & Tutorials*, vol. 26, no. 3, pp. 1560–1605, 2024.

[5] L. A. Iliadis, Z. D. Zaharis, S. Sotiroudis, P. Sarigiannidis, G. K. Karagiannidis, and S. K. Goudos, "The road to 6g: a comprehensive survey of deep learning applications in cell-free massive mimo communications systems," *EURASIP Journal on Wireless Communications and Networking*, vol. 2022, no. 1, p. 68, 2022.

[6] N. Rojhani and G. Shaker, "Comprehensive review: Effectiveness of mimo and beamforming technologies in detecting low rcs uavs," *Remote Sensing*, vol. 16, no. 6, p. 1016, 2024.

[7] M. T. Yalcinkaya, P. Sen, M. Ramzan, and G. P. Fettweiss, "Highly portable open source array phased antenna simulator," in *IEEE EUROCON 2023 - 20th International Conference on Smart Technologies*, pp. 450–454, 2023.

[8] G. A. Baduge, M. Vaezi, J. K. Dassanayake, M. Z. Hameed, E. Ollila, and S. A. Vorobyov, "Frequency range 3 for isac in 6g: Potentials and challenges," 2025.

[9] 5G Technology World, "Ims 5g summit: Design challenges remain, part 1." https://www.5gtechnologyworld.com/ims-5g-summit-design-challenges-remain-part-1/, 2025. Accessed: 2025-07-10.

[10] E. T. News, "Unlocking the potential of 6g fr3," 2025. Accessed: 2025-07-10.

[11] Cadence PCB Design & Analysis Blog, "Hybrid beamforming vs other types of beamforming." Cadence PCB Design & Analysis Blog, July2023 2023. https://resources.pcb.cadence.com/blog/2023-hybrid-beamforming-vs-other-types-of-beamforming.

[12] C. Andrews and A. C. Molnar, "A passive mixer-first receiver with digitally controlled and widely tunable rf interface," *IEEE Journal of Solid-State Circuits*, vol. 45, no. 12, pp. 2696–2708, 2010.

[13] L. Iotti, G. LaCaille, and A. M. Niknejad, "A 12mw 70-to-100ghz mixer-first receiver front-end for mm-wave massive-mimo arrays in 28nm cmos," in *2018 IEEE International Solid-State Circuits Conference - (ISSCC)*, pp. 414–416, 2018.

[14] S. Krishnamurthy, L. Iotti, and A. M. Niknejad, "Design of high-linearity mixer-first receivers for mm-wave digital mimo arrays," *IEEE Journal of Solid-State Circuits*, vol. 56, no. 11, pp. 3375–3387, 2021.

[15] P. Delos, S. Ringwood, and M. Jones, "Hybrid beamforming receiver dynamic range theory to practice." Analog Devices. [Online]. Available: https://www.analog.com/en/resources/technical-articles/hybrid-beamforming-receiver-dynamic-range.html, June 2022. Accessed: Aug. 21, 2025.

[16] A. Jamil, M. Z. Yusoff, and N. Yahya, "Current issues and challenges of mimo antenna designs," in *2010 International Conference on Intelligent and Advanced Systems*, pp. 1–5, 2010.

[17] M. T. Yalcinkaya, S. Kamal, P. Sen, and G. P. Fettweis, "The causal nexus between different feed networks and defected ground structures in multi-port mimo antennas," *Sensors*, vol. 24, no. 22, 2024.

[18] M.Tascioglu, "Antenna array simulator." https://github.com/Barkhausen-Institut/AntennaArraySimulator, 2021. Accessed: 2025-07-14.

[19] M.Tascioglu, "Antenna array simulator libraries." https://pypi.org/project/arrayfactor/, 2021. Accessed: 2025-07-14.

[20] C. A. Balanis, "Antenna theory," in *John Wiley&Sons*, Chapter 6, 2005.

[21] D. M. Pozar, *Microwave Engineering*. Hoboken, NJ: John Wiley & Sons, 4 ed., 2011.

[22] F. Gross, *Smart Antennas with MATLAB, Second Edition*. McGraw-Hill Education, 2015.